Simulating Non-Lambertian Phenomena Involving Linearly-Varying Luminaires

Min Chen James Arvo
California Institute of Technology, Pasadena, CA
{chen,arvo}@cs.caltech.edu

Abstract. We present a new technique for exactly computing glossy reflections and transmissions of polygonal Lambertian luminaires with linearly-varying radiant exitance. To derive the underlying closed-form expressions, we introduce a rational generalization of irradiance tensors and an associated recurrence relation. The generalized tensors allow us to integrate a useful class of rational polynomials over regions of the sphere; this class of rational polynomials can simultaneously account for the linear variation of radiant exitance across a planar luminaire and simple forms of non-Lambertian scattering. Applications include the computation of irradiance at a point, view-dependent reflections from glossy surfaces, and transmissions through glossy surfaces, where the scattering is limited to Phong distributions and the incident illumination is due to linearly-varying luminaires. In polyhedral environments, the resulting expressions can be exactly evaluated in quadratic time (in the Phong exponent) using dynamic programming or efficiently approximated in linear time using standard numerical quadrature. To illustrate the use of generalized irradiance tensors, we present a greatly simplified derivation of a previously published closed-form expression for the irradiance due to linearly-varying luminaires, and simulate Phong-like scattering effects from such emitters. The validity of our algorithm is demonstrated by comparison with Monte Carlo.

Keywords: Irradiance Tensors, Illumination, Glossy Reflection, Glossy Transmission.

1 Introduction

Deterministic rendering algorithms are often quite limited in the optical effects they simulate; for the most part they are limited to diffuse and pure specular effects. A common assumption is that of a uniform luminaire with constant radiance in all directions and positions, for which a wide assortment of closed-form expressions exist for computing the radiative exchange [10, 3, 15, 17] and some Phong-like scattering effects [2]. Unfortunately, these formulas rarely apply to non-uniform luminaires, especially *inhomogeneous* (or *spatially-varying*) luminaires, that is, area light sources whose radiant exitance varies as a function of position. This limitation stems from the difficulty of computing the integrals associated with spatially-varying luminaires. Unlike uniform luminaires, they generally cannot be expressed as a polynomial integrated over regions of the sphere.

Spatially-varying luminaires constitute an important class of light sources with immediate applications to higher-order finite element methods for global illumination, both for direct lighting [9] and final gathers from coarse global solutions [13]. Few methods exist for handling this type of luminaire aside from Monte Carlo integration. DiLaura [8] and the authors [6] have addressed the problem of computing the irradiance

at a point from spatially-varying luminaires with polynomially-varying radiant exitance. Both employed Stokes' theorem to convert the required surface integral to a boundary integral, and the latter approach leads to a closed-form solution for the irradiance due to a polygonal linearly-varying luminaire. As a continuation of our previous work [6], the contributions of this paper are as follows:

- A simpler derivation of the closed-form solution for the irradiance at a point due to a linearly-varying luminaire, using generalized irradiance tensors.
- The derivation of expressions for higher-order moments based on a class of rational polynomials over the sphere.
- An algorithm to evaluate these higher-order moments for simulating non-Lambertian scattering effects involving linearly-varying luminaires and non-diffuse surfaces, such as view-dependent glossy reflection and transmission.

Our approach generalizes *irradiance tensors* [2] to account for linearly-varying radiant exitance over the emitter. These new tensors are comprised of simple rational polynomials integrated over regions of the sphere. In particular, we address a limited subclass of rational polynomials corresponding to Phong distributions [12], which are shown to be well suited to simulate non-Lambertian phenomena involving linearly-varying luminaires. Using a recurrence formula derived for these *generalized irradiance tensors*, we demonstrate the exact integration of this subclass of rational polynomials in the case of polygonal emitters, and present a semi-analytical algorithm for their efficient computation. A similar approach using a tensor representation was previously used in analytically computing glossy reflection and transmission from uniform luminaires and the illumination from directional luminaires [2]. Our tensor generalization extends this previous method to handle linearly-varying luminaires as well, as shown in Figures 2a and 2b.

The remainder of the paper is organized as follows. Section 2 formulates the computation of some lighting effects involving linearly-varying luminaires and motivates our generalization of irradiance tensors in Section 3, which satisfies a recursive formula proved in Section 3.1. Based on this recurrence, we derive expressions for a simple class of rational polynomials in Section 3.2, which have immediate applications to several non-Lambertian simulations. We then discuss the exact evaluation of these expressions for polygonal emitters in Section 3.3. Finally, a semi-analytical algorithm is presented for their efficient computation in Section 3.4 and then used for image synthesis in Section 4.

2 Linearly-Varying Luminaires

In this section we examine the integrals arising in three non-Lambertian simulations involving linearly-varying luminaires; this will motivate our generalization of irradiance tensors.

Let $f(\mathbf{q}, \mathbf{u})$ denote the *radiance function* defined at all points $\mathbf{q} \in \mathbb{R}^3$ and all directions $\mathbf{u} \in \mathcal{S}^2$, the set of all unit vectors in $\mathbb{R}^3$. For fixed $\mathbf{q}$, this function simplifies to a *radiance distribution* $f(\mathbf{u})$ at $\mathbf{q}$. By default we assume that the point $\mathbf{q}$ we are interested in is at the origin. The goal of this paper is to characterize the radiance distribution function $f(\mathbf{u})$ due to a linearly-varying luminaire and to simulate various direct lighting and scattering effects from this type of emitter.

We begin with a brief recap of the formulation described in our previous work [6]. Suppose $\phi(\mathbf{x})$ is the *radiant exitance* of a luminaire at the point $\mathbf{x}$. The linearly-varying

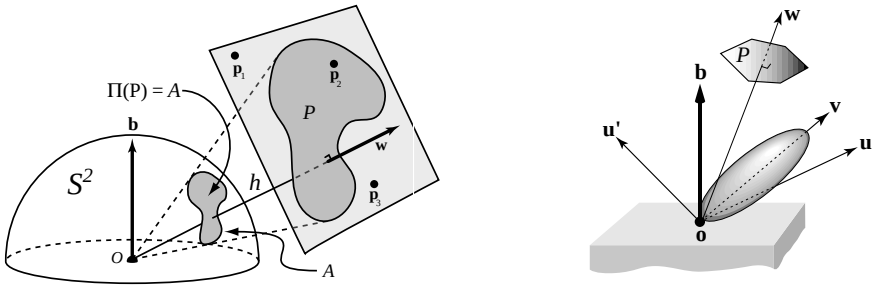

(a) (b)

Fig. 1. *(a) The radiance distribution function $f(\mathbf{u})$ at* **o** *due to a planar figure P with linearly varying radiant exitance is expressed as a simple rational polynomial over its spherical projection $\Pi(P) = A$. The radiant exitance variation is uniquely determined by any three non-collinear points $\mathbf{p}_1$, $\mathbf{p}_2$, and $\mathbf{p}_3$ on the luminaire plane. (b) Given a glossy surface with a simple BRDF defined in terms of a Phong exponent around the mirror reflection* **v**, *the reflected radiance along the view direction $\mathbf{u}'$ at* **o** *due to a linearly-varying luminaire P can be formulated as a simple rational polynomial integrated over regions of the sphere, that is, $\Pi(P)$.*

luminaires considered here are a class of planar emitters (not containing the origin) for which the function ϕ, mapping points on the plane to $\mathbb{R}$, is linear. Given any three non-collinear points $\mathbf{p}_1$, $\mathbf{p}_2$ and $\mathbf{p}_3$ on the luminaire with their associated radiant exitance values w_1, w_2 and w_3, the function ϕ can be expressed as

$$\phi(\mathbf{x}) \;=\; [w_1\ w_2\ w_3]\,[\mathbf{p}_1\ \mathbf{p}_2\ \mathbf{p}_3]^{-1}\,\mathbf{x}, \tag{1}$$

where $[\mathbf{p}_1\ \mathbf{p}_2\ \mathbf{p}_3]^{-1}\,\mathbf{x}$ is the barycentric coordinate vector of $\mathbf{x}$ with respect to $\mathbf{p}_1$, $\mathbf{p}_2$ and $\mathbf{p}_3$. Let h be the distance from the origin to the plane containing the luminaire and $\mathbf{w}$ denote the unit vector orthogonal to the plane, as shown in Figure 1a. We notice that the position vector $\mathbf{x}$ is related to its unit direction $\mathbf{u}$ from the origin by $\mathbf{x} = h\,\mathbf{u}/\langle \mathbf{w}, \mathbf{u}\rangle$, where $\langle\cdot,\cdot\rangle$ denotes the standard inner product. Consequently, the radiance distribution function $f(\mathbf{u})$ at the origin due to this Lambertian luminaire can be obtained by expressing $\mathbf{x}$ in equation (1) in terms of $\mathbf{u}$, yielding

$$f(\mathbf{u}) \;=\; \frac{\phi(\mathbf{x})}{\pi} \;=\; \frac{1}{\pi}\frac{\langle \mathbf{a}, \mathbf{u}\rangle}{\langle \mathbf{w}, \mathbf{u}\rangle}, \tag{2}$$

which is defined over the spherical projection of the luminaire at the origin, where the constant vector $\mathbf{a} = h\,[w_1\ w_2\ w_3]\,[\mathbf{p}_1\ \mathbf{p}_2\ \mathbf{p}_3]^{-1}$ encodes the linear variation.

Most emission and scattering effects involving linearly-varying luminaires can be formulated as weighted integrals of $f(\mathbf{u})$ given in (2) over spherical regions, which lead naturally to our tensor notion to be developed in Section 3.1. Let $\Pi(P)$ be the projection of a linearly-varying luminaire P onto the unit sphere about the origin, let $\mathbf{b}$ denote the receiver normal, and let σ measure the area on the sphere. We examine three different problems that each results in an integral with a rational integrand:

- The irradiance at the origin due to P is defined by

$$\Phi \;=\; \int_{\Pi(P)} f(\mathbf{u})\,\langle \mathbf{b}, \mathbf{u}\rangle\; d\sigma(\mathbf{u}) \;=\; \frac{1}{\pi}\int_{\Pi(P)} \frac{\langle \mathbf{a}, \mathbf{u}\rangle\,\langle \mathbf{b}, \mathbf{u}\rangle}{\langle \mathbf{w}, \mathbf{u}\rangle}\, d\sigma(\mathbf{u}). \tag{3}$$

- Given a glossy surface with a simple BRDF defined in terms of a Phong exponent by $\rho(\mathbf{u}' \rightarrow \mathbf{u}) \equiv c\left[-\mathbf{u}^{\mathrm{T}}(\mathbf{I}-2\mathbf{b}\mathbf{b}^{\mathrm{T}})\mathbf{u}'\right]^n$ for two directions $\mathbf{u}$ and $\mathbf{u}'$ shown in Figure 1b, the reflected radiance at a point on this surface along a view direction $\mathbf{u}'$ due to P is given by

$$f(\mathbf{u}') = \int_{\Pi(P)} \rho(\mathbf{u} \rightarrow \mathbf{u}') f(\mathbf{u}) \langle \mathbf{b}, \mathbf{u} \rangle \, d\sigma(\mathbf{u}) = \frac{c}{\pi} \int_{\Pi(P)} \frac{\langle \mathbf{v}, \mathbf{u} \rangle^n \langle \mathbf{a}, \mathbf{u} \rangle \langle \mathbf{b}, \mathbf{u} \rangle}{\langle \mathbf{w}, \mathbf{u} \rangle} \, d\sigma(\mathbf{u}), \quad (4)$$

  where $\rho(\mathbf{u} \rightarrow \mathbf{u}') = \rho(\mathbf{u}' \rightarrow \mathbf{u})$ due to reciprocity, and $\mathbf{v} = -(\mathbf{I}-2\mathbf{b}\mathbf{b}^{\mathrm{T}})\mathbf{u}'$ and n is the Phong exponent.
- By interpreting ρ above as a *bidirectional transmission distribution function* (BTDF) for a glossy surface, the transmitted radiance through this surface along a view direction $\mathbf{u}'$ due to P is represented by the same integral in (4), with $\mathbf{v}$ replaced by $-\mathbf{u}'$.

Note that the integrands in equations (3) and (4) are simple rational polynomials over the sphere. Simulating these non-Lambertian effects entails the computation of this type of integral.

3 Generalizing Irradiance Tensors

In this section we shall present new mathematical and computational tools for integrating some simple rational polynomials over regions of the sphere, which are required for the non-Lambertian simulations mentioned in the previous section.

3.1 Irradiance Tensors of Linearly-Varying Luminaires

As a natural generalization of the *radiation pressure tensor*, Arvo [2] introduced a tensor analogy of irradiance given by

$$\mathbf{T}^n(A) \equiv \int_A \mathbf{u} \otimes \cdots \otimes \mathbf{u} \, d\sigma(\mathbf{u}), \quad (5)$$

where $A \subset \mathcal{S}^2$ and the integrand is a n-fold tensor product. This tensor representation, known as the *irradiance tensor*, provides a useful vehicle for integrating *polynomial* functions over regions of the sphere. To concisely represent the *rational polynomial* integrals described in Section 2, we generalize the irradiance tensor shown in equation (5) to accommodate a denominator $\langle \mathbf{w}, \mathbf{u} \rangle$, resulting in a similar tensor form closely related to linearly-varying luminaires, defined as

$$\mathbf{T}^{n;1}(A, \mathbf{w}) \equiv \int_A \frac{\mathbf{u} \otimes \cdots \otimes \mathbf{u}}{\langle \mathbf{w}, \mathbf{u} \rangle} \, d\sigma(\mathbf{u}), \quad (6)$$

where we restrict $\mathbf{w}$ to be a unit vector such that $\langle \mathbf{w}, \mathbf{u} \rangle > 0$ for any $\mathbf{u} \in A$, and the orders of the numerator and the denominator are indicated respectively in the superscript $n; 1$. The elements of these tensors consist of all rational polynomials of the form $x^i y^j z^k / \langle \mathbf{w}, \mathbf{u} \rangle$ integrated over A, where $(x, y, z) \in \mathcal{S}^2$ and $i + j + k = n$.

Defined as surface integrals, the generalized irradiance tensors in equation (6) are computed by reducing them to boundary integrals, which yield closed-form solutions in polyhedral environments. Let $\mathbf{n}$ denote the outward-pointing normal of the boundary

curve ∂A. Using generalized Stokes' theorem [16], we have shown (see the Appendix) that $\mathbf{T}^{n;1}$ satisfies the recurrence relation

$$\mathbf{T}^{n;1}_{Ij}(A,\mathbf{w}) \;=\; \mathbf{w}_j\mathbf{T}^{n-1}_{I}(A) + \frac{1}{n}\left(\delta_{jm} - \mathbf{w}_j\mathbf{w}_m\right)\left[\sum_{k=1}^{n-1}\delta_{mI_k}\mathbf{T}^{n-2;1}_{I\backslash k}(A,\mathbf{w}) - \int_{\partial A}\frac{\mathbf{u}_I^{n-1}\mathbf{n}_m}{\langle\mathbf{w},\mathbf{u}\rangle}\,ds\right] \tag{7}$$

for $n > 0$, where δ_{ij} is the Kronecker delta. The irradiance tensor $\mathbf{T}^{n-1}$ can be further expanded by [2]

$$(n+1)\mathbf{T}^{n}_{Ij}(A) \;=\; \sum_{k=1}^{n-1}\delta_{jI_k}\mathbf{T}^{n-2}_{I\backslash k}(A) - \int_{\partial A}\mathbf{u}_I^{n-1}\mathbf{n}_j\,ds, \tag{8}$$

with $\mathbf{T}^{-1}(A) = 0$ and $\mathbf{T}^{0}(A) = \sigma(A)$, which is the solid angle subtended by the spherical region A. In equations (7) and (8), I is a $(n-1)$-index $(i_1, i_2, \ldots, i_{n-1})$, where $i_k \in \{1,2,3\}$ for $1 \le k \le n-1$. We define I_k as the kth subindex of I, $I\backslash k$ to be the $(n-2)$-index obtained by deleting the kth subindex, and Ij to be the n-index obtained by appending j after I. Finally, the recurrence relation (7) is completed by the base case

$$\mathbf{T}^{0;1}(A,\mathbf{w}) = \int_{\partial A}\frac{\ln\langle\mathbf{w},\mathbf{u}\rangle}{1-\langle\mathbf{w},\mathbf{u}\rangle^2}\langle\mathbf{w},\mathbf{n}\rangle\,ds, \tag{9}$$

where the integrand is defined as 0 when $\langle\mathbf{w},\mathbf{u}\rangle = 1$. The proof of equation (9) is supplied in the Appendix.

3.2 Rational Polynomials Integrated Over the Sphere

From equation (7) we may obtain expressions for a class of rational polynomials integrated over the sphere. Although it is these individual *scalar* elements that are required for image synthesis, the tensor formulation provides a powerful tool to represent a family of rational polynomials by means of tensor composition. Given an arbitrary region $A \subset \mathcal{S}^2$ and a sequence of axis vectors $\mathbf{v}_1, \mathbf{v}_2, \ldots$, we define a family of rational polynomials by

$$\tau^{p_1,p_2,\ldots;q}(A,\mathbf{v}_1,\mathbf{v}_2,\ldots;\mathbf{w}) \;\equiv\; \int_A\frac{\langle\mathbf{v}_1,\mathbf{u}\rangle^{p_1}\langle\mathbf{v}_2,\mathbf{u}\rangle^{p_2}\cdots}{\langle\mathbf{w},\mathbf{u}\rangle^{q}}\,d\sigma(\mathbf{u}) \tag{10}$$

for non-negative integers $p_1, p_2, \ldots, q$. When $q = 0$, this definition subsumes *axial moments* $\bar{\tau}^n(A,\mathbf{v})$ and *double-axis moments* $\bar{\bar{\tau}}^{n,1}(A,\mathbf{v}_1,\mathbf{v}_2)$ [2] as special cases, which correspond respectively to $\tau^{n;0}(A,\mathbf{v})$ and $\tau^{n,1;0}(A,\mathbf{v}_1,\mathbf{v}_2)$. Similarly, by specializing equation (10) to a small number of axes for $q = 1$, we may define three simple higher-order moments of $\mathbf{T}^{n;1}$, namely, $\tau^{n;1}(A,\mathbf{v};\mathbf{w})$, $\tau^{n,1;1}(A,\mathbf{v}_1,\mathbf{v}_2;\mathbf{w})$, and $\tau^{n,1,1;1}(A,\mathbf{v}_1,\mathbf{v}_2,\mathbf{v}_3;\mathbf{w})$. For simplicity, we shall only consider the case where one factor in the numerator is raised to the power n, and all the others are of order 1. These moments can be expressed as a tensor composition of $\mathbf{T}^{n;1}$ with copies of $\mathbf{v}_1$, $\mathbf{v}_2$ or $\mathbf{v}_3$. For example, $\tau^{n;1}(A,\mathbf{v};\mathbf{w}) = \mathbf{T}^{n;1}_{I}(A,\mathbf{w})(\mathbf{v}\otimes\cdots\otimes\mathbf{v})_I$. Here and throughout the

paper, the summation convention is employed, where repeated subscripts imply summation from 1 to 3, including multi-indices such as I [1, p.89]. We may derive the following recurrence relations from equation (7):

$$\begin{aligned}\tau^{n;1}(A,\mathbf{v};\mathbf{w}) &= \langle \mathbf{w},\mathbf{v}\rangle\, \bar{\tau}^{n-1}(A,\mathbf{v}) + \frac{\mathbf{v}^{\mathrm{T}}(\mathbf{I}-\mathbf{w}\mathbf{w}^{\mathrm{T}})}{n} \times \\ &\quad \left[(n-1)\tau^{n-2;1}(A,\mathbf{v};\mathbf{w})\,\mathbf{v} - \int_{\partial A} \mathbf{n}\frac{\langle \mathbf{v},\mathbf{u}\rangle^{n-1}}{\langle \mathbf{w},\mathbf{u}\rangle}\,ds\right] \quad (11)\\ \tau^{n,1;1}(A,\mathbf{v}_1,\mathbf{v}_2;\mathbf{w}) &= \langle \mathbf{w},\mathbf{v}_2\rangle\, \bar{\tau}^{n}(A,\mathbf{v}_1) + \frac{\mathbf{v}_2{}^{\mathrm{T}}(\mathbf{I}-\mathbf{w}\mathbf{w}^{\mathrm{T}})}{n+1} \times \\ &\quad \left[n\,\tau^{n-1;1}(A,\mathbf{v}_1;\mathbf{w})\,\mathbf{v}_1 - \int_{\partial A} \mathbf{n}\frac{\langle \mathbf{v}_1,\mathbf{u}\rangle^{n}}{\langle \mathbf{w},\mathbf{u}\rangle}\,ds\right] \quad (12)\\ \tau^{n,1,1;1}(A,\mathbf{v}_1,\mathbf{v}_2,\mathbf{v}_3;\mathbf{w}) &= \langle \mathbf{w},\mathbf{v}_3\rangle\, \bar{\bar{\tau}}^{n,1}(A,\mathbf{v}_1,\mathbf{v}_2) + \frac{\mathbf{v}_3{}^{\mathrm{T}}(\mathbf{I}-\mathbf{w}\mathbf{w}^{\mathrm{T}})}{n+2} \times \\ &\quad \big[n\tau^{n-1,1;1}(A,\mathbf{v}_1,\mathbf{v}_2;\mathbf{w})\,\mathbf{v}_1 + \tau^{n;1}(A,\mathbf{v}_1;\mathbf{w})\,\mathbf{v}_2 - \\ &\quad \int_{\partial A} \mathbf{n}\frac{\langle \mathbf{v}_1,\mathbf{u}\rangle^{n}\,\langle \mathbf{v}_2,\mathbf{u}\rangle}{\langle \mathbf{w},\mathbf{u}\rangle}\,ds\Big] \quad (13)\end{aligned}$$

In equation (11), we have $\tau^{0;1}(A,\mathbf{v};\mathbf{w}) = \mathbf{T}^{0;1}(A,\mathbf{w})$ and $\tau^{-1;1}(A,\mathbf{v};\mathbf{w}) = 0$; and the double-axis moment $\bar{\bar{\tau}}^{n,1}$ in (13) can be expressed in terms of axial moments by $\left(n\,\langle \mathbf{v}_1,\mathbf{v}_2\rangle\,\bar{\tau}^{n-1}(A,\mathbf{v}_1) - \int_{\partial A}\langle \mathbf{v}_1,\mathbf{u}\rangle^{n}\,\langle \mathbf{v}_2,\mathbf{n}\rangle\,ds\right)/(n+2)$ [2].

3.3 Exact Evaluation

Equations (11), (12) and (13) reduce the surface integrals $\tau^{n;1}$, $\tau^{n,1;1}$ and $\tau^{n,1,1;1}$ to boundary integrals of rational polynomials, and sums of axial moments and $\tau^{0;1}(=\mathbf{T}^{0;1})$. These moments can be integrated exactly whenever the resulting boundary integrals, axial moments and the base case $\tau^{0;1}$ can be. In this section we shall describe how these components can be evaluated in closed form when the region $A \subset \mathcal{S}^2$ is restricted to the spherical projection of a polygon P, which is a spherical polygon composed of segments of great arcs.

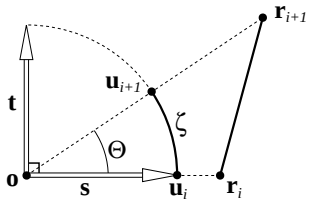

When A is a spherical polygon, the resulting boundary integrals can be evaluated along each edge ζ, which is greatly simplified due to the constant outward normal $\mathbf{n}$. We parameterize each edge ζ by $\mathbf{u}(\theta) = \mathbf{s}\cos\theta + \mathbf{t}\sin\theta$, where $\mathbf{s}$ and $\mathbf{t}$ are orthonormal vectors in the plane containing the edge and the origin, with $\mathbf{s}$ pointing toward the first vertex of the edge, as illustrated on the left. We shall define variables c and ϕ with respect to a vector $\mathbf{v}$ as:

$$c = \sqrt{\langle \mathbf{v},\mathbf{s}\rangle^2 + \langle \mathbf{v},\mathbf{t}\rangle^2}, \qquad (\cos\phi,\sin\phi) = \left(\frac{\langle \mathbf{v},\mathbf{s}\rangle}{c},\frac{\langle \mathbf{v},\mathbf{t}\rangle}{c}\right). \quad (14)$$

Exact evaluation of $\tau^{0;1}(A;\mathbf{w})$ $(=\mathbf{T}^{0;1}(A,\mathbf{w}))$ given in equation (9) requires us to integrate a scalar-valued function $\eta(\mathbf{w},\mathbf{u})$ defined by

$$\eta(\mathbf{w},\mathbf{u}) \equiv \frac{\ln\langle \mathbf{w},\mathbf{u}\rangle}{1-\langle \mathbf{w},\mathbf{u}\rangle^2} \quad (15)$$

along each edge ζ, which has been previously elaborated by the authors [6]. The solution is *closed form* except for one special function known as the Clausen integral [11]. As for the axial moment $\bar{\tau}^n$ about a unit vector $\mathbf{v}$, Arvo [2] has shown that it reduces to a one-dimensional integral by

$$n\bar{\tau}^{n-1}(A,\mathbf{v}) \;=\; \bar{\tau}^{p-1} - \int_{\partial A} \Big[\langle \mathbf{v},\mathbf{u}\rangle^{n-2} + \langle \mathbf{v},\mathbf{u}\rangle^{n-4} + \cdots + \langle \mathbf{v},\mathbf{u}\rangle^{p}\Big]\, \langle \mathbf{v},\mathbf{n}\rangle \; ds, \quad (16)$$

where $p = 0$ when n is even, and $p = 1$ when n is odd, and $\bar{\tau}^{-1}(A) = 0$ and $\bar{\tau}^0(A) = \sigma(A)$, which can be computed either from Girard's formula [4, 2] or a boundary integral formula for $\sigma(A)$ [6, 5]. From the above edge parameterization, the complete integral in equation (16) can be evaluated exactly in $\mathrm{O}(nk)$ time for a k-sided polygon, by computing the function $F(n,x,y) \equiv \int_x^y \cos^n\theta\, d\theta$ incrementally according to the following recurrence identity [2]:

$$F(n,x,y) \;=\; \frac{1}{n}\left[\cos^{n-1} y \sin y - \cos^{n-1} x \sin x + (n-1)F(n-2,x,y)\right]. \quad (17)$$

Finally, the boundary integrals appearing in formulas (11), (12) and (13) require us to compute two types of line integrals given by

$$B^n \;=\; \int_\zeta \frac{\langle \mathbf{v}_1,\mathbf{u}\rangle^n}{\langle \mathbf{w},\mathbf{u}\rangle}\, ds, \quad \text{and} \quad B^{n,1} \;=\; \int_\zeta \frac{\langle \mathbf{v}_1,\mathbf{u}\rangle^n \langle \mathbf{v}_2,\mathbf{u}\rangle}{\langle \mathbf{w},\mathbf{u}\rangle}\, ds,$$

which can be respectively evaluated using our edge parameterization as

$$B^n \;=\; \frac{c_1^n}{c}\int_{-\phi}^{\Theta-\phi} \frac{(\alpha_1\cos\theta + \beta_1\sin\theta)^n}{\cos\theta}\, d\theta, \quad (18)$$

$$B^{n,1} \;=\; \frac{c_1^n c_2}{c}\int_{-\phi}^{\Theta-\phi} \frac{(\alpha_1\cos\theta + \beta_1\sin\theta)^n(\alpha_2\cos\theta + \beta_2\sin\theta)}{\cos\theta}\, d\theta. \quad (19)$$

Here Θ is the arc length of ζ, and (c,ϕ), (c_1,ϕ_1), (c_2,ϕ_2) are variables defined for $\mathbf{w},\mathbf{v}_1,\mathbf{v}_2$ respectively using (14), and $\alpha_1,\beta_1,\alpha_2,\beta_2$ are given by

$$\alpha_i \;=\; \cos(\phi_i - \phi), \qquad \beta_i \;=\; \sin(\phi_i - \phi) \quad (i = 1,2).$$

Expanding the numerator using the binomial theorem, we can express B^n and $B^{n,1}$ in equations (18) and (19) in terms of integrals of the form

$$G(r,s,x,y) \;\equiv\; \int_x^y \sin^r\theta\, \cos^s\theta\, d\theta \quad (20)$$

for integers $r \geq 0$ and $s \geq -1$, yielding

$$B^n \;= \frac{c_1^n}{c}\sum_{k=0}^{n} \binom{n}{k} \alpha_1^{n-k}\beta_1^k\, G(k,n-k-1,x,y), \quad (21)$$

$$B^{n,1} = \frac{c_1^n c_2}{c}\sum_{k=0}^{n} \binom{n}{k} \alpha_1^{n-k}\beta_1^k\, \left[\alpha_2 G(k,n-k,x,y) + \beta_2 G(k+1,n-k-1,x,y)\right]. \quad (22)$$

The integral in (20) can be evaluated exactly in $\mathrm{O}(r+s)$ steps using the following recurrence relations:

$$G(r,s,x,y) = \frac{1}{r+s}\left[\sin^{r+1} y\cos^{s-1} y - \sin^{r+1} x\cos^{s-1} x + (s-1)G(r,s-2,x,y)\right],$$
$$G(r,s,x,y) = \frac{1}{r+s}\left[\sin^{r-1} x\cos^{s+1} x - \sin^{r-1} y\cos^{s+1} y + (r-1)G(r-2,s,x,y)\right],$$

where the base cases are

$$G(0,-1,x,y) = \ln\left(\frac{\tan(\pi/4+y/2)}{\tan(\pi/4+x/2)}\right), \quad G(1,0,x,y) = \cos x - \cos y,$$
$$G(1,-1,x,y) = \ln\left(\frac{\cos x}{\cos y}\right), \qquad G(0,0,x,y) = y - x.$$

Therefore, it takes $\mathrm{O}(n^2)$ time to exactly evaluate B^n or $B^{n,1}$ over one edge using equation (21) or equation (22).

3.4 Algorithms for Efficient Evaluation

Assuming that the evaluation of $\tau^{0;1}$ using the Clausen integral takes constant time [6], it then follows from the recurrence (11) that $\tau^{n;1}$ for a k-sided polygon may be computed exactly in $\mathrm{O}(n^3k)$ time, since we have shown that $\bar{\tau}^{n-1}$ and $\int_{\partial A} \mathbf{n}\langle\mathbf{v},\mathbf{u}\rangle^{n-1}/\langle\mathbf{w},\mathbf{u}\rangle\, ds$ can be evaluated in $\mathrm{O}(nk)$ and $\mathrm{O}(n^2k)$ respectively, by means of equations (16) and (21). However, we may reduce this complexity to $\mathrm{O}(n^2k)$ by reorganizing the terms obtained from the recurrence relation (11) and using dynamic programming [7, pp.301–328] to reuse many shared sub-expressions.

Let $d = \mathbf{v}^{\mathrm{T}}(\mathbf{I} - \mathbf{w}\mathbf{w}^{\mathrm{T}})\mathbf{v}$ and $k = \lfloor n/2 \rfloor$, the recurrence formula (11) leads to

$$\tau^{n;1}(A,\mathbf{v};\mathbf{w}) = T_1 + \frac{1}{n}\left[\langle\mathbf{w},\mathbf{v}\rangle\, T_2 - \mathbf{v}^{\mathrm{T}}(\mathbf{I}-\mathbf{w}\mathbf{w}^{\mathrm{T}})T_3\right]. \tag{23}$$

Defining $q = 0$ for even n and $q = -1$ for odd n, T_1, T_2 and T_3 above are given by

$$T_1 = d^{k-q}\left(\frac{q+1}{n}\right)\left(\frac{n-1}{n-2}\right)\left(\frac{n-3}{n-4}\right)\cdots\left(\frac{q+3}{q+2}\right)\tau^{q;1}, \tag{24}$$

$$T_2 = n\bar{\tau}^{n-1}(A,\mathbf{v}) + d\left(\frac{n-1}{n-2}\right)(n-2)\bar{\tau}^{n-3}(A,\mathbf{v}) + \cdots + d^{k-q-1}\left(\frac{n-1}{n-2}\right)\cdots\left(\frac{q+3}{q+2}\right)(q+2)\bar{\tau}^{q+1}(A,\mathbf{v}), \tag{25}$$

$$T_3 = \int_{\partial A}\frac{\mathbf{n}}{\langle\mathbf{w},\mathbf{u}\rangle}\left[\langle\mathbf{v},\mathbf{u}\rangle^{n-1} + d\left(\frac{n-1}{n-2}\right)\langle\mathbf{v},\mathbf{u}\rangle^{n-3} + \cdots + d^{k-q-1}\left(\frac{n-1}{n-2}\right)\left(\frac{n-3}{n-4}\right)\cdots\left(\frac{q+3}{q+2}\right)\langle\mathbf{v},\mathbf{u}\rangle^{q+1}\right] ds. \tag{26}$$

When $\mathbf{v}$ is normalized, we may use equation (16) to express T_2 as

$$T_2 = \left[1 + d\left(\frac{n-1}{n-2}\right) + \cdots + d^{k-q-1}\left(\frac{n-1}{n-2}\right)\cdots\left(\frac{q+3}{q+2}\right)\right]\bar{\tau}^{p-1} -$$

$$\sum_{i=1}^{k} \left[\langle \mathbf{v}, \mathbf{n} \rangle \, S(n-2, c, d, -\phi, \Theta - \phi) \right], \tag{27}$$

where $\mathbf{n}$, Θ and c, ϕ given in (14) all depend on the edge ζ_i ($1 \leq i \leq k$), and p is defined as in (16). Here $S(n-2, c, d, x, y)$ is a sum of the integrals $F = \int_x^y \cos^n \theta \, d\theta$ of different exponents, given by

$$\begin{aligned} & c^{n-2} F(n-2, x, y) + \left[1 + d \left(\frac{n-1}{n-2} \right) \right] c^{n-4} F(n-4, x, y) + \cdots \\ + & \left[1 + d \left(\frac{n-1}{n-2} \right) + \cdots + d^{k-1} \left(\frac{n-1}{n-2} \right) \cdots \left(\frac{p+3}{p+2} \right) \right] c^p F(p, x, y), \end{aligned} \tag{28}$$

which can be computed incrementally in linear time using the identity (17). To compute the weighted sum of integrals B^n with n ranging from $q+1$ to $n-1$ required for T_3 using (21), we may precompute and cache n^2 values of $G(r, s, x, y)$ for $0 \leq r \leq n-1$ and $-1 \leq s \leq n-2$. This common technique known as *dynamic programming* reduces the cubic complexity for the exact evaluation of T_3 down to quadratic. Consequently, $\tau^{n;1}$ may be evaluated analytically using equation (23) in $\mathrm{O}(n^2 k)$ time for a k-sided polygon. From recursive formulas (12) and (13), we may also compute $\tau^{n,1;1}$ and $\tau^{n,1,1;1}$ exactly in quadratic time, where a great deal of redundant computations involving the functions F and G may be avoided by allowing the routines for $\tau^{n;1}$ to return some additional higher-order terms in the series of T_2 and T_3. Furthermore, observing the common coefficients 1, $\frac{n-1}{n-2}$, $\frac{(n-1)(n-3)}{(n-2)(n-4)}$, $\ldots$ occurring in equations (24), (25) and (26), another optimization is to cache this series of values before evaluating T_1, T_2, T_3. All these optimizations significantly reduce the constant related to the quadratic complexity. The complete pseudo-code and details for computing $\tau^{n;1}$ and $\tau^{n,1;1}$, $\tau^{n,1,1;1}$ for a polygon are available as a technical report [5].

Another option for speeding up the computation is to approximate T_3 using numerical quadrature; this is particularly effective as T_3 has the highest computational cost, yet is typically very small in magnitude compared to T_1 and T_2. In terms of accuracy, this approach is preferable to approximating the original integral using two-dimensional quadrature, as one-dimensional quadrature rules are more robust and more amenable to higher-order methods. By computing the powers of $\langle \mathbf{v}, \mathbf{u} \rangle$ in equation (26) incrementally through repeated multiplication for each sampled $\mathbf{u}$, the complete integral (26) can be evaluated within $\mathrm{O}(ln)$ time for each edge, where l is the number of samples used in the quadrature rule. For fixed l, this semi-analytical algorithm allows us to compute $\tau^{n;1}$ of a k-sided polygon in linear time. We have used this approach in combination with the extended trapezoidal rule to generate the images shown in Section 4.

4 Non-Lambertian Effects from Linearly-Varying Luminaires

Generalized irradiance tensors $\mathbf{T}^{n;1}$ and those moments expressed as a class of rational polynomials integrated over the sphere are well suited to the computation of emission and scattering features due to linearly-varying luminaires, especially for polygonal environments with Phong-like reflection (or transmission) distributions. Therefore, the expressions and procedures given in previous sections may be applied to the simulation of illumination, glossy reflection and glossy transmission involving linearly-varying luminaires, which will be described next.

4.1 Irradiance due to a Linearly-Varying Luminaire

Generalized irradiance tensors provide a more elegant means of deriving the closed-form solution for the irradiance due to a linearly-varying luminaire reported previously by the authors [6]. Our previous approach, which was based on Taylor expansion and a formula derived for *triple-axis moments*, is quite tedious.

According to definitions (10) and (6), we express the irradiance integral (3) as

$$\Phi \;=\; \frac{1}{\pi}\tau^{1,1;1}(A,\mathbf{a},\mathbf{b};\mathbf{w}) \;=\; \frac{1}{\pi}\mathbf{T}^{2;1}_{ij}(A,\mathbf{w})\,\mathbf{a}_i\mathbf{b}_j. \tag{29}$$

Using equations (7), (8) and (9), $\mathbf{T}^{2;1}$ reduces to a boundary integral as follows:

$$\begin{aligned}\mathbf{T}^{2;1}_{ij} &= \mathbf{w}_j\mathbf{T}^1_i + \frac{1}{2}\left(\delta_{jm}-\mathbf{w}_j\mathbf{w}_m\right)\left[\delta_{im}\mathbf{T}^{0,1} - \int_{\partial A}\frac{\mathbf{u}_i\mathbf{n}_m}{\langle\mathbf{w},\mathbf{u}\rangle}\,ds\right]\\ &= -\frac{1}{2}\int_{\partial A}\left[\delta_{ik}\mathbf{w}_j - \left(\delta_{jm}-\mathbf{w}_j\mathbf{w}_m\right)\left(\delta_{im}\mathbf{w}_k\;\eta - \frac{\delta_{km}\mathbf{u}_i}{\langle\mathbf{w},\mathbf{u}\rangle}\right)\right]\mathbf{n}_k\;ds, \end{aligned}\tag{30}$$

where η is given by equation (15). Combining equations (29) and (30), we arrive at the general boundary integral for the irradiance at the origin [6]

$$\Phi \;=\; -\frac{1}{2\pi}\int_{\partial A}\mathbf{M}_{ijk}\mathbf{a}_i\mathbf{b}_j\mathbf{n}_k\;ds, \tag{31}$$

where the 3-tensor $\mathbf{M}$, which depends on $\mathbf{w}$ and $\mathbf{u}$, is defined as

$$\mathbf{M}_{ijk}(\mathbf{w},\mathbf{u}) \;=\; \delta_{ik}\mathbf{w}_j + \left(\delta_{jm}-\mathbf{w}_j\mathbf{w}_m\right)\left(\frac{\delta_{km}\mathbf{u}_i}{\langle\mathbf{w},\mathbf{u}\rangle} - \delta_{im}\mathbf{w}_k\;\eta\right).$$

As we have demonstrated earlier [6], the integral (31) leads to a closed-form solution involving a single special function known as the Clausen integral for polygonal emitters.

4.2 Phong-like Glossy Reflection and Transmission

As mentioned in Section 2, the reflected radiance along the view direction $\mathbf{u}'$ on a glossy surface with Phong-like BRDF due to a linearly-varying luminaire can be formulated as a surface integral shown in equation (4), which is equivalent to $f(\mathbf{u}') = c\,\tau^{n,1,1;1}(A,\mathbf{v},\mathbf{b},\mathbf{a};\mathbf{w})/\pi$, with n as the Phong exponent. Thus the procedures described in Section 3.4 can be implemented inside a ray tracer to simulate such glossy reflection effects. For a scene consisting of a linearly-varying luminaire P and a glossy surface Q, each pixel color is determined by the pseudo-code *GlossyReflection*, where f and n are the reflectivity and Phong exponent of Q, and Q_c, P_c, B_c denote the colors for Q, P, and the background, respectively. The technique is demonstrated in the top row of Figure 3 using a variety of exponents to simulate surfaces with varying finishes. In order to efficiently handle two color variations superimposed on the luminaire shown in Figure 3, we separate the vector $\mathbf{a}$ encoding the linear variation from equation (13) and rewrite $\tau^{n,1,1;1}$ as an inner product of $\mathbf{a}$ and a vector-valued function $\mathbf{t}(A,\mathbf{v},\mathbf{b},\mathbf{w})$ given by

$$\begin{aligned}\mathbf{t}(A,\mathbf{v},\mathbf{b},\mathbf{w}) &= \mathbf{w}\bar{\bar{\tau}}^{n,1}(A,\mathbf{v},\mathbf{b}) + \frac{\mathbf{I}-\mathbf{w}\mathbf{w}^{\mathrm{T}}}{n+2}\Big[n\tau^{n-1,1;1}(A,\mathbf{v},\mathbf{b};\mathbf{w})\,\mathbf{v}+\\ &\qquad \tau^{n;1}(A,\mathbf{v};\mathbf{w})\,\mathbf{b} - \int_{\partial A}\mathbf{n}\frac{\langle\mathbf{v},\mathbf{u}\rangle^n\langle\mathbf{b},\mathbf{u}\rangle}{\langle\mathbf{w},\mathbf{u}\rangle}\,ds\Big],\end{aligned}\tag{32}$$

GlossyReflection(**Eye**, Q, f, n, P, Q_c, P_c, B_c)

for each pixel ξ **do**
  Ray $R \leftarrow$ *ray cast from* **Eye** *to* ξ
  q $\leftarrow$ *the first intersection point of the ray* R
  if q is on the luminaire P
    $PixelColor \leftarrow P_c$
  else if q is on the glossy surface Q
    b $\leftarrow$ *surface normal at* **q**
    $\mathbf{u}' \leftarrow$ *direction of* R
    $\mathbf{v} \leftarrow (\mathbf{I} - 2\mathbf{b}\mathbf{b}^{\mathrm{T}})\mathbf{u}'$
    w $\leftarrow$ *unit vector from* **q** *orthogonal to* P
    a $\leftarrow$ *vector encoding the linear variation of* P
    $A \leftarrow$ *spherical projection of* P *at* **q**
    $s \leftarrow \tau^{n,1,1;1}(A, \mathbf{v}, \mathbf{b}, \mathbf{a}; \mathbf{w})$ *(See Section 3.4)*
    $PixelColor \leftarrow f * [s * P_c + (1 - s) * B_c] + (1 - f) * Q_c$
  else
    $PixelColor \leftarrow B_c$
  endif
endfor

which amortizes the computation cost for more than one color variations. In Figure 2, our analytical glossy reflection is compared with a Monte Carlo solution based on 64 samples per pixel, where the samples are stratified and distributed according to the Phong lobe (this is a form of importance sampling). The analytical solution closely matches the Monte Carlo estimate but with the advantage of eliminating statistical noise; in this example it is even slightly faster than Monte Carlo method.

Nearly the same strategy can be used to compute glossy transmission of linearly-varying luminaires by choosing **v** in equation (32) as the reversed view direction $-\mathbf{u}'$, which is now located on the other side of the transparent material. The bottom row of Figure 3 shows three images depicting a frosted glass fish tank, with different finishes specified by different Phong exponents.

The performance of our analytical approach is determined by such factors as the image resolution, the Phong exponent, and the luminaire complexity. All timings shown in Figure 2 and Figure 3 were done using a SGI Onyx2 with a 300 MHZ MIPS R12000 processor, and an image resolution of 200×200.

5 Conclusions

We have presented a number of new closed-form expressions for computing the illumination from luminaires with linearly-varying radiant exitance as well as glossy reflections and transmissions of such luminaires. These expressions are derived using a simple rational generalization of irradiance tensors, and can be evaluated analytically in $\mathrm{O}(n^2k)$ time for a k-sided polygonal luminaire using dynamic programming, where n is related to the glossiness of the surface. The exact solution depends on a single well-behaved special function known as the Clausen integral. We have also presented a semi-analytical algorithm for evaluating these expressions efficiently for the purpose of simulating glossy reflection and glossy transmission of linearly-varying luminaires. A similar approach is possible for general polynomials [5], although the recurrence formulas have not yet yielded a computationally tractable evaluation strategy.

Acknowledgements

This work was supported by a Microsoft Research Fellowship and NSF Career Award CCR9876332. Special thanks to Al Barr, Peter Schröder, Mark Meyer and Eitan Grinspun for helpful comments.

Appendix: Proofs of Equation (7) and Equation (9)

The proof of equation (7) parallels that of equation (8) shown by Arvo [1, pp. 84–87]. It is done by applying Stokes' Theorem to change the boundary integral on the right to a surface integral, which can be accomplished in four steps:

Step 1**:** Let $r = ||\,\mathbf{r}\,||$. Notice that $\mathbf{n}\ ds = \mathbf{r} \times\ d\mathbf{r}/r^2$ and $\mathbf{u} = \mathbf{r}/r$, we may rewrite the boundary integral on the right hand side in terms of the position vector $\mathbf{r}$ and its derivatives:

$$\int_{\partial A} \frac{\mathbf{u}_I^{n-1}\mathbf{n}_m}{\langle \mathbf{w}, \mathbf{u}\rangle}\, ds \;=\; \int_{\partial A} \frac{\varepsilon_{mpl}\mathbf{r}_I^{n-1}\mathbf{r}_p\ d\mathbf{r}_l}{\langle \mathbf{w}, \mathbf{r}\rangle\, r^n} \;=\; \int_{\partial A} B_{Iml}\, d\mathbf{r}_l, \tag{33}$$

where ε_{ijk} is the permutation symbol [1, pp.69–70] and B is a $(n+1)$-order tensor B given by

$$B_{Iml} \;=\; \frac{\varepsilon_{mpl}\mathbf{r}_I^{n-1}\mathbf{r}_p}{\langle \mathbf{w}, \mathbf{r}\rangle\, r^n}.$$

Step 2**:** To convert the boundary integral in equation (33) into a surface integral using Stokes' theorem, we must compute the partial derivative of B_{Iml} with respect to $\mathbf{r}_s$, denoted by $B_{Iml,s}$. It follows from the chain rule that

$$B_{Iml,s} = \varepsilon_{mpl}\left(\frac{\partial}{\partial \mathbf{r}_s}\left[\frac{1}{\langle \mathbf{w}, \mathbf{r}\rangle}\right]\left[\frac{\mathbf{r}_p\mathbf{r}_I^{n-1}}{r^n}\right] + \left[\frac{1}{\langle \mathbf{w}, \mathbf{r}\rangle}\right]\frac{\partial}{\partial \mathbf{r}_s}\left[\frac{\mathbf{r}_p\mathbf{r}_I^{n-1}}{r^n}\right]\right) = \varepsilon_{mpl}\left[A_1 + A_2\right].$$

where A_1, A_2 are given by

$$A_1 \;=\; -\frac{\mathbf{w}_s\mathbf{r}_p\mathbf{r}_I^{n-1}}{\langle \mathbf{w}, \mathbf{r}\rangle^2\, r^n}, \quad A_2 \;=\; \frac{\delta_{ps}\mathbf{r}_I^{n-1} + \mathbf{r}_p\mathbf{r}_{I,s}^{n-1}}{\langle \mathbf{w}, \mathbf{r}\rangle\, r^n} - n\frac{\mathbf{r}_s\mathbf{r}_p\mathbf{r}_I^{n-1}}{\langle \mathbf{w}, \mathbf{r}\rangle\, r^{n+2}}.$$

Thus, we have

$$\begin{aligned}
\int_{\partial A} B_{Iml}\, d\mathbf{r}_l \;&=\; \int_A B_{Iml,s}\ d\mathbf{r}_s \wedge\ d\mathbf{r}_l \\
&=\; \int_A B_{Iml,s}\left[\frac{d\mathbf{r}_s \wedge\ d\mathbf{r}_l - \ d\mathbf{r}_l \wedge\ d\mathbf{r}_s}{2}\right] \\
&=\; \int_A \varepsilon_{qsl}\varepsilon_{mpl}\left[A_1 + A_2\right]\left[\frac{\varepsilon_{qht}\ d\mathbf{r}_h \wedge\ d\mathbf{r}_t}{2}\right].
\end{aligned} \tag{34}$$

The transformation above follows from anti-commutativity of the wedge product [14][1, p. 68] and the tensor identity $\varepsilon_{\,qsl}\varepsilon_{qht} \;=\; \delta_{sh}\delta_{tl} - \delta_{st}\delta_{lh}$.

Step 3**:** Applying the above identity to the two terms in equation (34), we get

$$\begin{aligned}
\varepsilon_{qsl}\varepsilon_{mpl}A_1 &= \frac{\mathbf{r}_I^{n-1}}{\langle \mathbf{w},\mathbf{r}\rangle^2 r^n}\left[\delta_{qm}\langle \mathbf{w},\mathbf{r}\rangle - \mathbf{w}_m\mathbf{r}_q\right], \\
\varepsilon_{qsl}\varepsilon_{mpl}A_2 &= \frac{1}{\langle \mathbf{w},\mathbf{r}\rangle}\left[\frac{\delta_{qm}\mathbf{r}_I^{n-1}}{r^n} - \frac{\mathbf{r}_q\mathbf{r}_{I,m}^{n-1}}{r^n} + n\frac{\mathbf{r}_q\mathbf{r}_m\mathbf{r}_I^{n-1}}{r^{n+2}}\right].
\end{aligned}$$

Consequently, equation (34) simplifies to

$$\int_A \left[\frac{\mathbf{w}_m\mathbf{r}_I^{n-1}}{\langle \mathbf{w},\mathbf{r}\rangle^2 r^{n-3}} - \frac{\sum_{k=1}^{n-1}\delta_{mI_k}\mathbf{r}_{I\backslash k}^{n-2}}{\langle \mathbf{w},\mathbf{r}\rangle r^{n-3}} + n\frac{\mathbf{r}_m\mathbf{r}_I^{n-1}}{\langle \mathbf{w},\mathbf{r}\rangle r^{n-1}}\right]\left[\frac{\varepsilon_{qht}\mathbf{r}_q\, d\mathbf{r}_h \wedge\ d\mathbf{r}_t}{2r^3}\right]. \quad (35)$$

Step 4**:** Multiplying equation (35) by $(\delta_{jm} - \mathbf{w}_j\mathbf{w}_m)/n$ and representing the surface integral in terms of solid angle $d\sigma(\mathbf{u}) \equiv -\varepsilon_{qst}\mathbf{r}_q\, d\mathbf{r}_s \wedge\ d\mathbf{r}_t/2r^3$ [16, p. 131], we attain

$$-\frac{1}{n}\left(\delta_{jm} - \mathbf{w}_j\mathbf{w}_m\right)\int_{\partial A} B_{Iml}\, d\mathbf{r}_l \;=\; \frac{1}{n}\left(\delta_{jm} - \mathbf{w}_j\mathbf{w}_m\right)\sum_{k=1}^{n-1}\delta_{mI_k}\mathbf{T}_{I\backslash k}^{n-2;1} + \mathbf{w}_j\mathbf{T}_I^{n-1} - \mathbf{T}_{Ij}^{n;1},$$

which verifies equation (7).

The steps to prove equation (9) are almost identical to those used in the proof of equation (7) described above, so we only show the difference here. Corresponding to equations (33) and (34), we have

$$\int_{\partial A}\frac{\ln\langle \mathbf{w},\mathbf{u}\rangle}{1-\langle \mathbf{w},\mathbf{u}\rangle^2}\langle \mathbf{w},\mathbf{n}\rangle\, ds \;=\; \int_{\partial A} B_l\, d\mathbf{r}_l \;=\; \int_A \varepsilon_{qml}B_{l,m}\left[\frac{\varepsilon_{qst}\, d\mathbf{r}_s \wedge\ d\mathbf{r}_t}{2}\right], \quad (36)$$

where the vector B is given by

$$B_l \;=\; \varepsilon_{kpl}\mathbf{w}_k\frac{\ln\langle \mathbf{w},\mathbf{u}\rangle}{1-\langle \mathbf{w},\mathbf{u}\rangle^2}\cdot\frac{\mathbf{r}_p}{r^2} \;=\; \varepsilon_{kpl}\mathbf{w}_k\eta\frac{\mathbf{r}_p}{r^2},$$

and its derivative with respect to $\mathbf{r}_m$ is computed from the chain rule by

$$B_{l,m} \;=\; \varepsilon_{kpl}\mathbf{w}_k\left[\eta\frac{\partial}{\partial\mathbf{r}_m}\left(\frac{\mathbf{r}_p}{r^2}\right) + \left(\frac{\partial\eta}{\partial\mathbf{r}_m}\right)\frac{\mathbf{r}_p}{r^2}\right].$$

Here, we have

$$\frac{\partial}{\partial\mathbf{r}_m}\left(\frac{\mathbf{r}_p}{r^2}\right) = \frac{\delta_{pm}r^2 - 2\mathbf{r}_p\mathbf{r}_m}{r^4},\quad \frac{\partial\eta}{\partial\mathbf{r}_m} = \frac{r^2 - \langle \mathbf{w},\mathbf{r}\rangle^2 + 2\langle \mathbf{w},\mathbf{r}\rangle^2\ln\langle \mathbf{w},\mathbf{u}\rangle}{\left(r^2 - \langle \mathbf{w},\mathbf{r}\rangle^2\right)^2}\left[\frac{r^2\mathbf{w}_m}{\langle \mathbf{w},\mathbf{r}\rangle} - \mathbf{r}_m\right].$$

After simplification, we attain

$$\begin{aligned}
\varepsilon_{qml}\varepsilon_{kpl}\mathbf{w}_k\eta\frac{\partial}{\partial\mathbf{r}_m}\left(\frac{\mathbf{r}_p}{r^2}\right) &= \frac{\mathbf{r}_q}{r^3}\left[2\eta\langle \mathbf{w},\mathbf{u}\rangle\right], \\
\varepsilon_{qml}\varepsilon_{kpl}\mathbf{w}_k\left(\frac{\partial\eta}{\partial\mathbf{r}_m}\right)\frac{\mathbf{r}_p}{r^2} &= -\frac{\mathbf{r}_q}{r^3}\left[\frac{1}{\langle \mathbf{w},\mathbf{u}\rangle} + 2\eta\langle \mathbf{w},\mathbf{u}\rangle\right].
\end{aligned}$$

Equation (9) then follows easily by representing the right hand side of equation (36) in terms of solid angle $d\sigma(\mathbf{u})$, as shown in the previous derivation.

References

1. James Arvo. *Analytic Methods for Simulated Light Transport*. PhD thesis, Yale University, December 1995.
2. James Arvo. Applications of irradiance tensors to the simulation of non-Lambertian phenomena. In *Computer Graphics* Proceedings, Annual Conference Series, ACM SIGGRAPH, pages 335–342, August 1995.
3. Daniel R. Baum, Holly E. Rushmeier, and James M. Winget. Improving radiosity solutions through the use of analytically determined form-factors. *Computer Graphics*, 23(3):325–334, July 1989.
4. Marcel Berger. *Geometry*, volume 2. Springer-Verlag, New York, 1987. Translated by M. Cole and S. Levy.
5. Min Chen. *Mathematical Methods for Image Synthesis*. PhD thesis, California Institute of Technology, June 2001. http://www.cs.caltech.edu/~chen/papers/thesis/phd_thesis.ps.gz.
6. Min Chen and James Arvo. A closed-form solution for the irradiance due to linearly-varying luminaires. In B. Péroche and H. Rushmeier, editors, *Rendering Techniques 2000*. Springer-Verlag, New York, 2000.
7. Thomas H. Cormen, Charles E. Leiserson, and Ronald L. Rivest. *Introduction to Algorithms*. McGraw-Hill, New York, 1990.
8. David L. DiLaura. Non-diffuse radiative transfer 3: Inhomogeneous planar area sources and point receivers. *Journal of the Illuminating Engineering Society*, 26(1), 1997.
9. Nicholas Holzschuch and Franccois X. Sillion. Accurate computation of the radiosity gradient for constant and linear emitters. In *Proceedings of the Sixth Eurographics Workshop on Rendering*, Dublin, Eire, June 1995.
10. John R. Howell. *A Catalog of Radiation Configuration Factors*. McGraw-Hill, New York, 1982.
11. Leonard Lewin. *Dilogarithms and associated functions*. Macdonald, London, 1958.
12. Bui Tuong Phong. Illumination for computer generated pictures. *Communications of the ACM*, 18(6):311–317, June 1975.
13. Mark C. Reichert. A two-pass radiosity method driven by lights and viewer position. Master's thesis, Cornell University, January 1992.
14. M. Schreiber. *Differential Forms: A Heuristic Introduction*. Springer-Verlag, New York, 1984.
15. Peter Schröder and Pat Hanrahan. On the form factor between two polygons. In *Computer Graphics* Proceedings, Annual Conference Series, ACM SIGGRAPH, pages 163–164, August 1993.
16. Michael Spivak. *Calculus on Manifolds*. Benjamin/Cummings, Reading, Massachusetts, 1965.
17. Michael M. Stark and Richard F. Riesenfeld. Exact illumination in polygonal environments using vertex tracing. In B. Péroche and H. Rushmeier, editors, *Rendering Techniques 2000*. Springer-Verlag, New York, 2000.

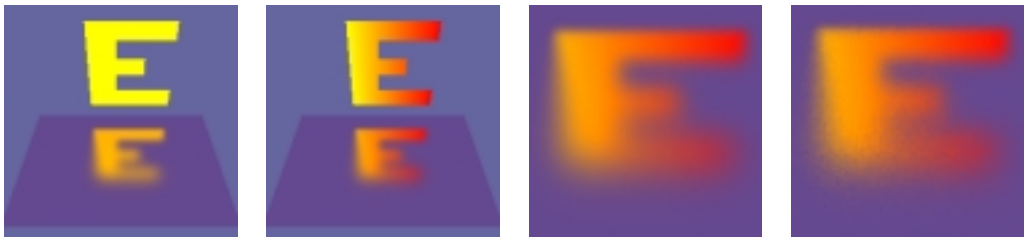

(a) (b) (c) (2.1m) (d) (2.5m)

Fig. 2. *A simple test scene of analytical glossy reflection involving a glossy surface with a Phong exponent of* 200 *and an E-shaped luminaire whose radiant exitance is uniform (a) and linearly-varying with respect to position (b). The closeup images of the reflection on the floor were computed analytically (c) and by Monte Carlo method with approximately the same amount of time, using stratified and importance sampling and* 64 *samples per pixel (d).*

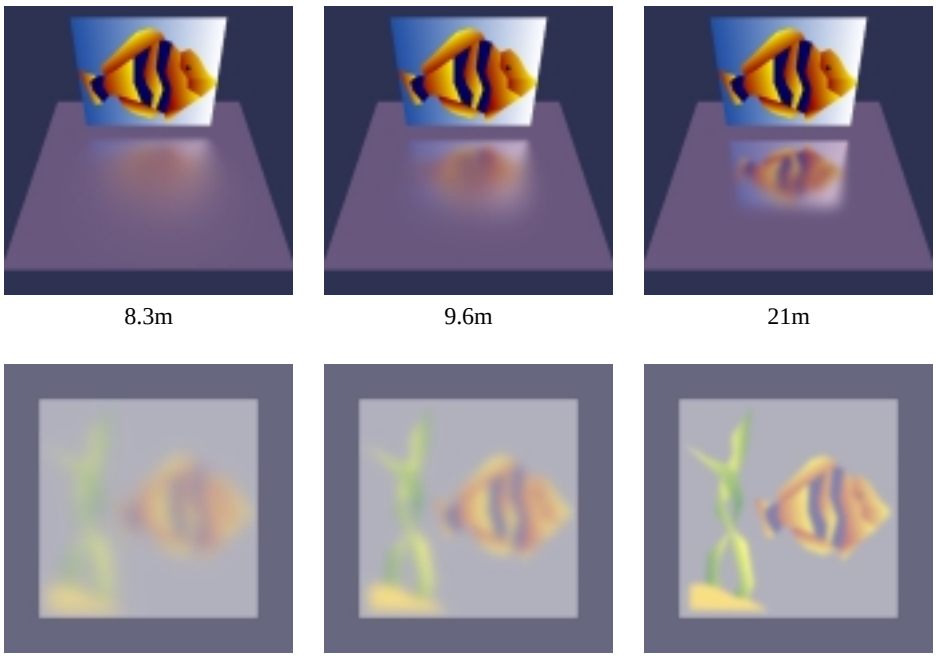

8.3m 9.6m 21m

11.5m 12.1m 15.4m

Fig. 3. *(Top) Glossy reflection of a stained glass window with linearly-varying colors, where the Phong exponents are* 15, 50 *and* 300 *from left to right. (Bottom) Glossy transmission through a frosted glass fish tank, where the tropical fish and the seaweed are superimposed with linearly-varying colors. From left to right, the Phong exponents are* 5, 15, *and* 65, *respectively. Refraction is not considered here. The numbers beneath each image indicate the computation time in minutes.*